

where v_i are the velocities and γ_i the inverse scale lengths of each species. The constants in the second formula are

$$A = [\gamma_{\text{H}_2\text{O}}/(\gamma_{\text{H}_2} - \gamma_{\text{H}_2\text{O}})] [1 + (\gamma_{\text{H}_2\text{O}})/(\gamma_{\text{OH}} - \gamma_{\text{H}_2\text{O}})]$$

$$B = -A + [\gamma_{\text{H}_2\text{O}}\gamma_{\text{OH}}/(\gamma_{\text{OH}} - \gamma_{\text{H}_2\text{O}})(\gamma_{\text{H}_2} - \gamma_{\text{OH}})]$$

and $C = -A - B$.

10. M. R. Combi, A. H. Delsemme, *Astrophys. J.* **237**, 633 (1980).
11. The 1-AU scale lengths and velocities appropriate for solar maximum conditions were $\Lambda_{\text{H}_2\text{O}} = 6.6 \times 10^4$ km, $\Lambda_{\text{OH}} = 1.75 \times 10^5$ km, $\Lambda_{\text{H}_1} = 3 \times 10^7$ km, $v_{\text{H}_1} = 20$ km s⁻¹, $\Lambda_{\text{H}_2} = 1.2 \times 10^7$ km, and $v_{\text{H}_2} = 8$ km s⁻¹. Because of the large FOV, the inner production region of the H coma is not resolved, and so the calculations are more sensitive to the H velocities than to parent lifetimes.
12. M. C. Festou, *Astron. Astrophys.* **95**, 69 (1981).
13. M. R. Combi et al., *Earth Moon Planets* **79**, 275 (1997).
14. The model neglects several minor effects like radiation pressure, Greenstein effect, and the dependence of scale lengths of different species on variations of the solar irradiation flux. Their combined contribution to the results can be estimated from given error margins.
15. This is similar but not equal to the active area and is defined as $A = LQr^2/[N_A F_S(1 - A_V)]$, where $L = 50$ kJ mol⁻¹ is the latent heat of water for sublimation, r is the heliocentric distance in AU, $N_A = 6.022 \times 10^{23}$ mol⁻¹ (the Avogadro constant), $F_S = 1365$ W m⁻² (the solar constant), and $A_V = 0.03$ (the assumed Bond albedo of the nucleus). See, e.g., (23), for a discussion of this definition.
16. D. Bockelée-Morvan et al., *Science* **292**, 1339 (2001).
17. T. L. Farnham et al., *Science* **292**, 1348 (2001).
18. H. A. Weaver et al., *Science* **292**, 1329 (2001).
19. The continuous size distribution is discretized by dividing it into classes of fragments of the same size. For the purpose of evaluation here, five particle-size groupings were used. For each class the total water-production rate Q_i of the class i can be obtained by solving the dissipation equation

$$dQ_i/dt = - (9u \sqrt{\pi N_i} / \rho) [N_i F_S (1 - A_V) / Lr^2]^{3/2} [Q_i(t)]^{1/2}$$
 where $u = 1.66 \times 10^{-27}$ kg is the atomic mass unit, $N_i = N_0 b^{i/m}$, $i = 0, \dots, m$ the number of fragments in the respective class, $b = N_m / N_0$, and ρ is the bulk density, which can be determined if N_0 is known or vice versa. The total water-production rate is thus $Q_{\text{H}_2\text{O}}(t) = \sum Q_i(t)$.

20. The initial mass on 24 July corresponds to the integrated loss of water after that point, and the power-law exponent determines the shape of the slope. It can thus be seen from Fig. 4 that the model reproduces these two quantities.
21. Z. Sekanina, *Astron. Astrophys.* **318**, L5 (1997).
22. W. H. Press, B. P. Flannery, S. A. Teukolsky, W. T. Vetterling, *Numerical Recipes* (Cambridge Univ. Press, New York, 1986), pp. 52–64.
23. H. U. Keller, in *Physics and Chemistry of Comets*, W. F. Huebner, Ed. (Springer-Verlag, Berlin, 1990), pp. 18–21.
24. SOHO is an international cooperative mission of the European Space Agency and NASA. SWAN was financed by Centre National d'Études Spatiales (France) with support from CNRS and by Teknologian Keskittämiskeskus (National Technology Agency, Finland) and the Finnish Meteorological Institute. J.T.T.M. was supported by the Academy of Finland. M.R.C. acknowledges support from the SOHO Guest Investigator Programme. We thank the authors of the other C/LINEAR papers in this issue for sharing their results before publication, especially H. A. Weaver for constructive comments.

20 March 2001; accepted 19 April 2001

HST and VLT Investigations of the Fragments of Comet C/1999 S4 (LINEAR)

H. A. Weaver,^{1*} Z. Sekanina,² I. Toth,³ C. E. Delahodde,^{4†} O. R. Hainaut,⁴ P. L. Lamy,⁵ J. M. Bauer,⁶ M. F. A'Hearn,⁷ C. Arpigny,⁸ M. R. Combi,⁹ J. K. Davies,¹⁰ P. D. Feldman,¹ M. C. Festou,¹¹ R. Hook,¹² L. Jorda,⁵ M. S. W. Keesey,² C. M. Lisse,^{13‡} B. G. Marsden,¹⁴ K. J. Meech,⁶ G. P. Tozzi,¹⁵ R. West¹²

At least 16 fragments were detected in images of comet C/1999 S4 (LINEAR) taken on 5 August 2000 with the Hubble Space Telescope (HST) and on 6 August with the Very Large Telescope (VLT). Photometric analysis of the fragments indicates that the largest ones have effective spherical diameters of about 100 meters, which implies that the total mass in the observed fragments was about 2×10^9 kilograms. The comet's dust tail, which was the most prominent optical feature in August, was produced during a major fragmentation event, whose activity peaked on UT 22.8 ± 0.2 July 2000. The mass of small particles (diameters less than about 230 micrometers) in the tail was about 4×10^8 kilograms, which is comparable to the mass contained in a large fragment and to the total mass lost from water sublimation after 21 July 2000 (about 3×10^8 kilograms). HST spectroscopic observations during 5 and 6 July 2000 demonstrate that the nucleus contained little carbon monoxide ice (ratio of carbon monoxide to water is less than or equal to 0.4%), which suggests that this volatile species did not play a role in the fragmentation of C/1999 S4 (LINEAR).

Cometary fragmentation events provide an opportunity to gather direct information on the internal structure and composition of cometary nuclei, which is difficult to obtain in any other way. Optical imaging observations of comets suggest that their nuclei split at a rate of at least once every hundred years (1). These fragmentations are generally grouped into two categories: events that seem to be caused by tidal interactions with a nearby large object, such as for comet D/Shoemaker-Levy 9 after its close

approach to Jupiter in 1992, and disruptions that occur for no apparent reason, although breakup due to fast rotation is a tenable explanation in at least some of these cases (2–4). The nucleus of comet C/1999 S4 (LINEAR), hereafter called C/LINEAR, underwent multiple fragmentations during its recent apparition, culminating in the complete disruption of its nucleus during the latter part of July 2000 (5). C/LINEAR did not pass particularly close to any major planetary body during its current apparition, so tidal

disruption is apparently not responsible for its fragmentation.

C/LINEAR was discovered on 27 September 1999 (all dates are expressed in universal time) by the Lincoln Near Earth Asteroid Research (LINEAR) program (6) at a heliocentric distance of 4.3 astronomical units (AU) (1 AU = 1.496×10^{11} m is the average Earth-Sun distance). The comet was apparently on its first visit to the inner solar system from the Oort cloud, a vast reservoir of $\sim 10^{12}$ comets that surrounds the Sun (7, 8), and reached perihelion on 26 July 2000 at a heliocentric distance of 0.77 AU. We observed C/LINEAR both pre-

¹Department of Physics and Astronomy, Johns Hopkins University, 3400 North Charles Street, Baltimore, MD 21218–2686, USA. ²Jet Propulsion Laboratory, 4800 Oak Grove Drive, Pasadena, CA 91109, USA. ³Konkoly Observatory, Post Office Box 67, Budapest H-1525, Hungary. ⁴European Southern Observatory, Alonso de Cordova 3107, Santiago, Chile. ⁵Laboratoire d'Astronomie Spatiale du CNRS, BP 8, 13376 Marseille, Cedex 12, France. ⁶Institute for Astronomy, University of Hawaii, 2680 Woodlawn Drive, Honolulu, HI 96822, USA. ⁷Department of Astronomy, University of Maryland, College Park, MD 20742, USA. ⁸Institut d'Astrophysique, Université de Liège, B-4000 Liège, Belgium. ⁹Space Physics Research Laboratory, University of Michigan, 2455 Hayward Street, Ann Arbor, MI 48109–2143, USA. ¹⁰Joint Astronomy Centre, Hilo, HI 96720, USA. ¹¹Observatoire Midi-Pyrénées, 14 avenue Edouard Belin, F-31400 Toulouse, France. ¹²European Southern Observatory, Karl-Schwarzschild-Strasse 2, D-85748 Garching, Germany. ¹³Space Telescope Science Institute, 3900 San Martin Drive, Baltimore, MD 21218, USA. ¹⁴Smithsonian Astrophysical Observatory, 60 Garden Street, Cambridge, MA 02138, USA. ¹⁵Osservatorio Astrofisico di Arcetri, Largo E. Fermi 5, I-50125, Florence, Italy.

*To whom correspondence should be addressed.

†Present address: Laboratoire d'Astronomie Spatiale du CNRS, BP 8, 13376 Marseille, Cedex 12, France.

‡Present address: Department of Astronomy, University of Maryland, College Park, MD 20742, USA.

COMET C/LINEAR

and post-perihelion, using several different facilities (Table 1).

Our first observations of C/LINEAR were made during 5 through 7 July 2000 with the Space Telescope Imaging Spectrograph (STIS) (9) on the Hubble Space Telescope (HST). During the observations on 5 July, the comet was on the rising portion of a strong activity outburst in which the comet's brightness in a 0.15 arc sec by 0.15 arc sec region centered on the nucleus (0.15 arc sec projects to ~ 90 km at the comet) increased by a factor of nearly 1.5 in ~ 4 hours. When we observed the comet 1 day

later, the brightness had fallen to $\sim 90\%$ of the first value measured on 5 July and continued declining until our final observation on 7 July, when the brightness was only one-seventh of its peak value on 5 July. In an image taken on 7 July, we detected at least one fragment located ~ 460 km in projected distance tailward from the main nucleus. This was the only reported pre-perihelion detection of a fragment near C/LINEAR, and it was possibly released from the nucleus during the outburst detected 2 days earlier. If so, and if the fragment started with zero velocity and was moving exactly along the

Sun-comet line (the Sun-comet-Earth angle was between 74° and 79°), the nongravitational acceleration, produced by jetting forces from sublimating ices, was $\sim 3 \times 10^{-3}$ to 7×10^{-3} times that of solar gravity (10), which is an order of magnitude larger than the acceleration deduced for several fragments observed during August 2000 (see later discussion).

After the reported disintegration of the comet's nucleus in late July 2000, we made ground-based observations of C/LINEAR each day during 2 through 5 August 2000, using the University of Hawaii 2.2-m telescope on the Mauna Kea Observatory (11), but only R-band images from 4 August are discussed here. Although no fragments could be detected in these images, we used them to construct a model for the production of the comet's dust tail (12). From the measured celestial position angle of the tail axis on 4 August ($98.0^\circ \pm 0.2^\circ$, J2000 equinox), we derive that the outburst event producing the dust tail peaked on 22.8 ± 0.2 July 2000. The shape of the tail demonstrates that the event had a rapid rise and tapered off more slowly, but we have not yet attempted to quantify this description. Analysis of the spatial brightness profiles along and across the tail shows that the position of peak intensity is dominated by particles having $\beta \approx 0.01$, where β is the ratio of solar radiation pressure to solar gravity (13). This value of β corresponds to particles ~ 230 μm in diameter, assuming that their density is 0.5 g cm^{-3} . We estimate that the total R magnitude of the tail is $\sim 8.6 \pm 0.2$, and from this we derive that the total mass of the dust tail is $\sim (4.1 \pm 0.8) \times 10^8$ kg, assuming that the particles have a geometric albedo of 4% and using a phase correction factor of 2 in brightness (14). Our estimate depends on the phase-law dependence for the dust scattering because the observations were conducted at a phase angle of 88.9° , and extreme choices could change our mass estimate by a factor of ~ 2 in either direction. We have only considered the contribution from grains having a product of density and diameter smaller than $\sim 2 \text{ g cm}^{-2}$ ($\beta > 6 \times 10^{-5}$), so the actual mass will be larger if pebblesized and larger particles contribute. The mass in the dust tail is comparable to the total mass of gas released after 21 July 2000 ($\sim 3 \times 10^8$ kg) (15, 16). If all of the mass in the dust tail were put into a single spherical object having a density of 0.5 g cm^{-3} (17), its diameter would be ~ 120 m, which suggests that the breakup event of 22.8 July 2000 resulted in the complete disintegration of one or more large fragments.

On 5 August 2000, we observed C/LINEAR with the HST and used the Wide Field and Planetary Camera 2 (WFPC2) (18) to obtain images of the comet (Fig. 1) at three different locations: the Planetary Camera (PC) charge-coupled device (CCD) was cen-

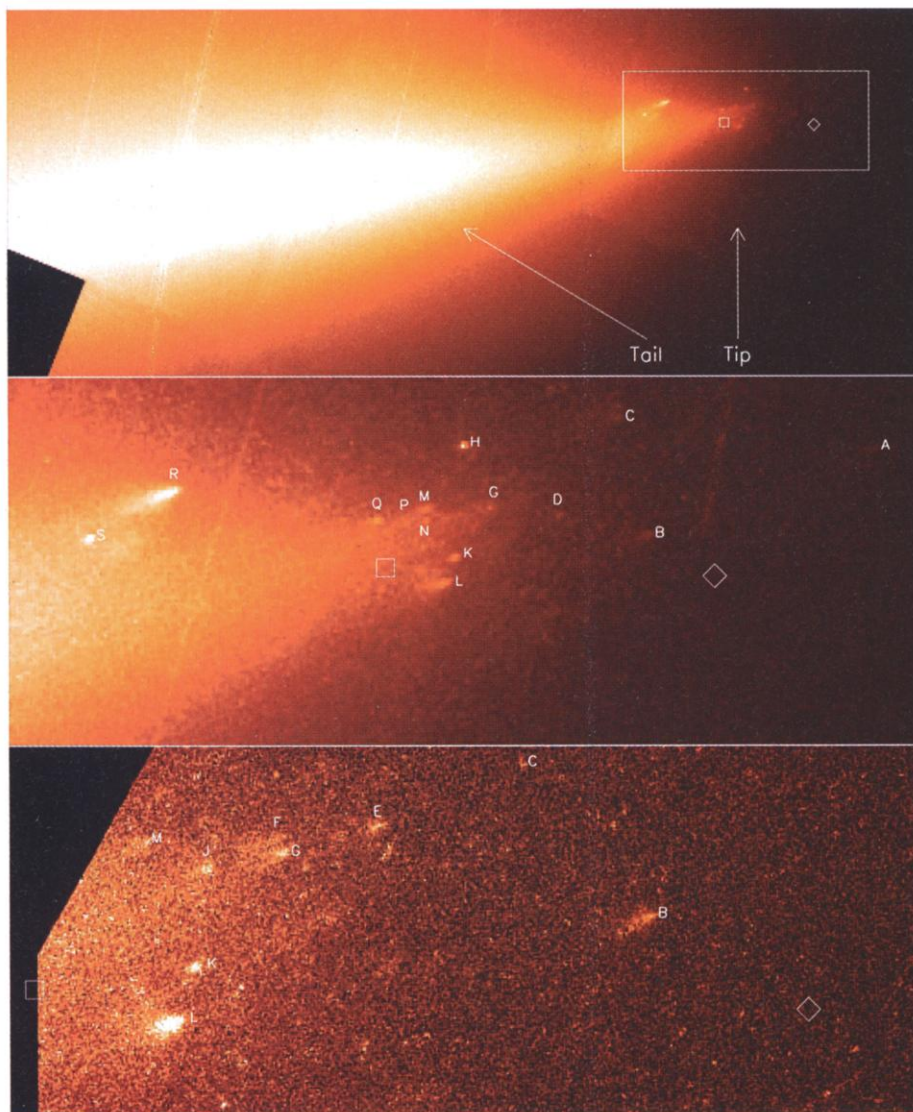


Fig. 1. HST WFPC2 images of C/LINEAR. **(Top)** A mosaic of two images taken in WFC mode on 5.38 and on 5.45 August 2000, demonstrating that the bright tail dominated the comet's optical emission. However, near the western tip of the tail (within the outlined box; celestial north is straight up and east is to the left), one can see clear evidence for individual fragments. **(Middle)** This region is magnified, showing that the fragments resembled miniature comets with their own comae and tails. **(Bottom)** Our highest resolution image of the tip region, taken in PC mode on 5.18 August 2000. The fragments are labeled with their letter names in the middle and bottom panels. The diamonds give the predicted position of the original nucleus using the JPL-87 orbit solution, and the squares show the predicted position of the nucleus using the JPL-95 orbit solution (19). Their separation, 19.3 arc sec on this date, serves as a scale bar for each of the displayed images. The nearly vertical streaks are trails from stars passing through the field that were not completely removed during image processing.

COMET C/LINEAR

tered on the predicted position of the nucleus (19), on a region 80 arc sec tailward of the nucleus, and on a location 160 arc sec tailward. The most prominent optical feature of C/LINEAR was the tail of dust extending antisunward of the predicted position of the nucleus, which is also nearly due east. The westernmost edge of the tail forms a relatively sharp tip that could be discerned even from modest-sized ground-based telescopes. HST's high-spatial-resolution images show that the tip actually consists of ~12 fragments, each resembling a miniature comet with its own coma and tail. In addition, a few fragments lie substantially west of the tip, close to the predicted location of the original nucleus and in the region where one would generally expect to find the most massive fragments (19).

Approximately 37 hours after the first HST observations on 5 August 2000, we observed C/LINEAR on 6 August, using the Very Large Telescope (VLT) (20). Those images revealed even more fragments (~16) after special image-processing techniques were applied to enhance the unresolved sources (Fig. 2) (21). VLT observations were also made on 9 and 14 August, but no fragments could be seen in the raw images, and image processing did not yield any definite detections (20). We estimate that the brightest fragment must have faded by a factor of ~10 between 6 and 14 August and the faintest fragment must have faded by at least a factor of ~2.

Because the identifications of the fragments from one image to another are sometimes ambiguous, we assigned a separate lettering scheme for the HST PC image centered on the predicted position of the nucleus, for the HST Wide Field Camera (WFC) image that contains the tip region (this image was taken ~6.5 hours after the PC image), and for the VLT image. Tentative correspondences were made among the fragments (Table 2), and their relative positions were plotted (Fig. 3). We identified two pairs of fragments that originally might have been part of the same object. Assuming that our identifications are correct, we measured the increase in the separation between the pairs over the observed time period and applied a model (4) to estimate both the separation times and the accelerations of the fragments (Table 2). Our best fit models indicate that these fragments probably separated sometime between late June and mid-July 2000 and that their nongravitational accelerations were $\sim 3 \times 10^{-4}$ to 5×10^{-4} of the acceleration of solar gravity (10). These separation times are earlier than what is commonly referred to as the disruption time of C/LINEAR (i.e., on or about 22 July 2000) and indicate that the fragmentation had a progressive nature extending over a period of at least 1 month. However, our results do not preclude the possibility that many of the fragments were produced during the late-July disruption event.

Table 1. Log of observations. The STIS (9) and the WFPC2 (18) are instruments on the National Aeronautics and Space Administration/European Space Agency HST. The Tek2K CCD camera was used at the University of Hawaii (UH) 2.2-m telescope (11). The FORS1 was used at the ESO's VLT (20). r_h and Δ are the comet's heliocentric and geocentric distances, respectively, and ϕ is the phase angle in degrees (Sun-comet-Earth angle).

| Start-stop dates (UT) | Observatory/instrument | r_h (AU) | Δ (AU) | ϕ (deg) | Filter/grating | Exposure times (s) | Comments |
|-----------------------|------------------------|------------|---------------|--------------|-------------------|-----------------------------------|--------------------------------------|
| 5.78–5.94 Jul 2000 | HST/STIS | 0.86 | 0.82 | 74.6 | F28x50LP G140L | 30 × 4 1800, 1800, 1440 | Rising activity; CO detection |
| 6.73–6.89 Jul 2000 | HST/STIS | 0.85 | 0.78 | 76.9 | F28x50LP G230L | 30 × 4 1800, 1800, 1440 | Declining activity; OH monitoring |
| 7.66–7.96 Jul 2000 | HST/STIS | 0.85 | 0.74 | 79.3 | F28x50LP | 30 × 1 | Low activity; fragment in tail |
| 4.25–4.30 Aug 2000 | UH/Tek2K | 0.79 | 0.66 | 88.9 | R band | 90 × 3 | Dust tail imaging |
| 5.17–5.47 Aug 2000* | HST/WFPC2 | 0.79 | 0.69 | 86.0 | F675W | 1100 × 2, 1000 × 2, 2,1100 × 2 | ≥ 14 fragments |
| 6.98–7.00 Aug 2000 | VLT/FORS1 | 0.80 | 0.75 | 81.5 | R band | 558, 600, 500 | ≥ 16 fragments |
| 9.98–10.00 Aug 2000 | VLT/FORS1 | 0.82 | 0.86 | 74.1 | R band | 400 × 4 | Poor conditions; ≤ 3 fragments |
| 14.98–15.00 Aug 2000 | VLT/FORS1 | 0.86 | 1.04 | 63.5 | R band | 500 × 4 | No fragments |

*There were pointings at three different locations (19).

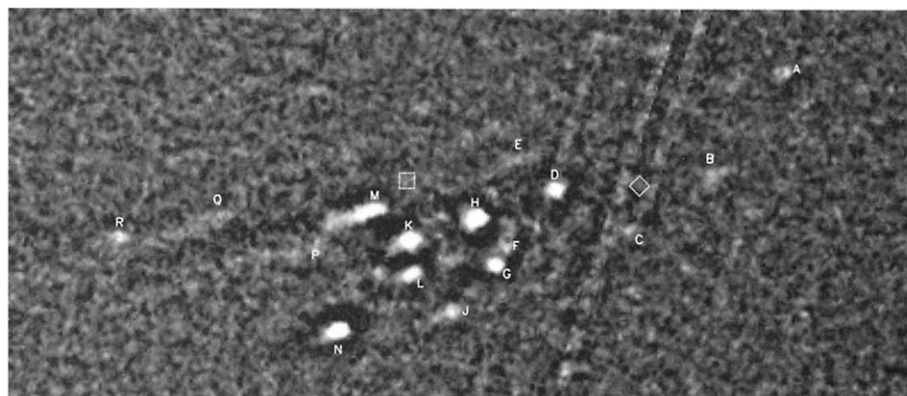
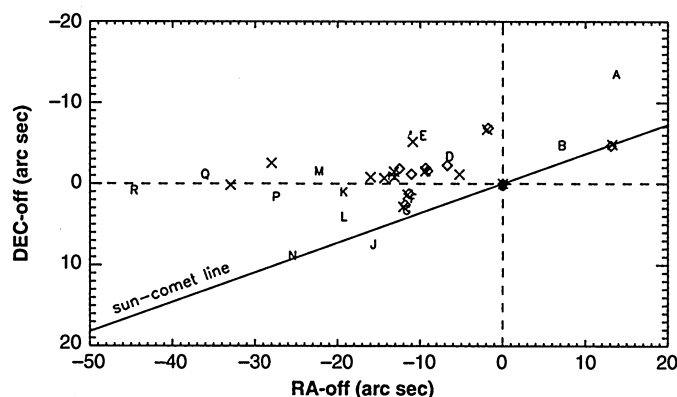


Fig. 2. VLT image of C/LINEAR taken on 6.99 August 2000. Three individual images were combined and then processed with both unsharp masking and wavelet filtering (21). At least 16 fragments were detected, and they are labeled with their letter names. Celestial north is straight up, and east is to the left. The diamond gives the predicted position of the original nucleus with the JPL-87 orbit solution, and the square shows the predicted position of the nucleus with the JPL-95 orbit solution (19). Their separation was 20.3 arc sec on this date. The nearly vertical streaks are trails from stars passing through the field that were not completely removed during image processing.

Fig. 3. Locations of the C/LINEAR fragments. The relative positions (DEC-off, offset in declination from the origin; RA-off, offset in right ascension from the arbitrary origin) of the fragments are plotted as derived from the HST PC observations taken on 5.18 August 2000 (diamonds), from the HST WFC observations taken on 5.45 August 2000 (crosses), and from the VLT observations taken on 6.99 August 2000 (letters). Celestial north is straight up, and east is to the left. The origin is arbitrarily selected to coincide with fragments B_{PC} , B_{WFC} , and C_{VLT} (the caption for Table 2 explains the naming convention). The line connecting the comet and the Sun, as projected on the sky, is also shown, and the Sun is to the west. The letters overlap the other symbols in some cases (e.g., C, F, G, and H).



COMET C/LINEAR

The accelerations and implied lifetimes (~ 3 to 6 weeks) derived by us for the two pairs of fragments are consistent with those observed in other disrupted comets (4).

The presence of nongravitational accelerations, dust comae, and tails for the fragments strongly suggests that they were at least partially covered with ice and that the sublimation of this ice carried dust particles away from the surface to produce the coma; that is, each of the fragments was essentially a miniature comet. Using two different techniques that have been employed to extract the magnitudes of cometary nuclei from WFPC2 images of other comets (22, 23), we performed a detailed photometric analysis of the spatial brightness distribution around each of the 10 fragments detected in the PC image. The two methods generally yielded consistent results for the nuclear magnitudes, and in all cases

we present the average values from these two independent techniques (Table 2). An example of the fit with one of the methods (22) is shown in Fig. 4. We converted the magnitudes into sizes (24), assuming that the objects are spherical, their geometric albedo is 4%, and their brightness follows a linear phase law of $0.04 \text{ mag deg}^{-1}$ (mag, magnitudes). The largest objects have effective diameters of $\sim 100 \text{ m}$, with a possible systematic error of a factor of ~ 2 in either direction (25). We note that some of the fragments appear to have secondary components (e.g., B, E, L, and possibly G), and models that contain multiple objects provide somewhat better fits to the observations in those cases. However, the observed signals for the frag-

ments are so faint that further analysis is required before any definitive statements can be made regarding the multiplicity of the fragments.

Using our size estimates, we calculated the masses of the fragments (Table 2), assuming that they have a density of 0.5 g cm^{-3} (17). The total mass contained in the 10 fragments listed in Table 2 is $\sim 2 \times 10^9 \text{ kg}$, which is almost an order of magnitude larger than the total mass lost from water sublimation after 21 July 2000 [$\sim 3 \times 10^8 \text{ kg}$ (15, 16)]. Inclusion of the other fragments, and of possible companions to the fragments listed in Table 2, will raise the total mass of the fragments, but probably not by more than a factor of 2. A single spherical object having a density of 0.5 g cm^{-3} and a mass of $2 \times 10^9 \text{ kg}$ would have a diameter of $\sim 200 \text{ m}$, which presumably is a lower limit to the original size of C/LINEAR's nucleus. Owing to various sources of systematic error (25), our estimate for the total mass of the fragments is uncertain by about an order of magnitude, so we cannot say with certainty that most of the mass of C/LINEAR ended up in the large fragments observed in the HST and VLT images.

A spherical 50-m-diameter object with a geometric albedo of 4% and a phase law that varies as $0.04 \text{ mag deg}^{-1}$ would have an R magnitude of 27.6, which means that an inactive nucleus of this size would be near the detectability limit of the HST and the VLT. We note also that 50- to 100-m objects with little ice would have low gas production rates, so the presence of such bodies does not violate the upper limits on gas production in August 2000 derived from other observations (15, 16). Presumably, objects covering a broad range of sizes were produced during the breakup of C/LINEAR, but our observations are mainly sensitive to those at the extreme ends of the size spectrum, i.e., to micrometer-sized dust and the largest fragments. Therefore, a substantial fraction of the leftover mass from C/LINEAR may be in intermediate-sized objects, from centimeter-sized particles to $\sim 50\text{-m}$ objects, that escape detection by optical observations.

Ultraviolet spectra of C/LINEAR were obtained by STIS during 5 through 7 July 2000 (26). We detected emissions from CO and OH and from these data derive an abundance ratio of $\text{CO}/\text{H}_2\text{O} \leq 0.4\%$ (27), which is smaller than the values observed in other comets, sometimes by more than an order of magnitude (28). CO has a sublimation temperature under solar nebula conditions of $\sim 25 \text{ K}$ (29) and has frequently been invoked both as the source of cometary activity at large heliocentric distances and as a possible trigger for short-term cometary activity outbursts. The lack of appreciable amounts of CO in the nucleus of C/LINEAR apparently rules out any important role for CO in the comet's fragmentations and temporal outbursts.

Table 2. C/LINEAR fragments. Fragments of C/LINEAR were separately detected in images taken with the WFPC2 in PC mode on 5 August 2000, with the WFPC2 in WFC mode on 5 August 2000, and with the VLT on 6 August 2000; separate letter designation systems have been defined in each case. Approximately 16 fragments were detected in the VLT image, with letter names from A through R, but omitting I and O. Approximately 14 fragments were detected in the WFC image, with letter names from A to S, but omitting E, F, I, and O. Approximately 10 fragments were detected in the PC image, with letter names from A to M, but omitting D, H, and I. In all cases, the order of the letters reflects their astronomical right ascension, from west (A) to east (S). m_r is the derived R-band magnitude of each fragment after removal of any coma contribution, and this has been converted to an effective spherical diameter (d_N), assuming that the geometric albedo is 4% and that the brightness follows a linear phase law of $0.04 \text{ mag deg}^{-1}$. The size has been converted to a mass by assuming that each fragment has a density of 0.5 g cm^{-3} . As discussed in the text (25), the sizes and masses possibly have large systematic errors.

| Fragment names | | | m_r | d_N (m) | Mass (10^8 kg) |
|----------------|-----|-----|-------|--------------|-------------------------------|
| PC | WFC | VLT | | | |
| A | A | B | 27.3 | 50 | 0.4 |
| B | B | C | 26.3 | 80 | 1.5* |
| C | C | | 26.0 | 100 | 2.3 |
| E | | | 26.2 | 90 | 1.7 |
| F | | | 26.8 | 70 | 0.8 |
| G | G | | 26.1 | 90 | 2.0 |
| J | | | 25.7 | 110 | 3.4 |
| K | K | K | 26.0 | 100 | 2.3 |
| L | L | L | 25.5 | 120 | 4.5† |
| M | M | H | 26.0 | 100 | 2.3‡ |

*Closest to the predicted position of the original nucleus. †Values refer to the brighter component of a pair of objects; possible fragment of $A_{PC} = A_{WFC} = B_{VLT}$; $a_{ng} = 39 \pm 8$, where a_{ng} is the nongravitational acceleration of the fragment due to the jetting effect from gases and dust leaving its surface, in units of 10^{-5} of the acceleration due to solar gravity (10); $T_{sep} = 2 \pm 6$ July 2000, where T_{sep} is the estimated date when the fragment separated from its parent. ‡Possible fragment of $B_{PC} = B_{WFC} = C_{VLT}$; $a_{ng} = 34 \pm 8$; $T_{sep} = 13 \pm 3$ July 2000.

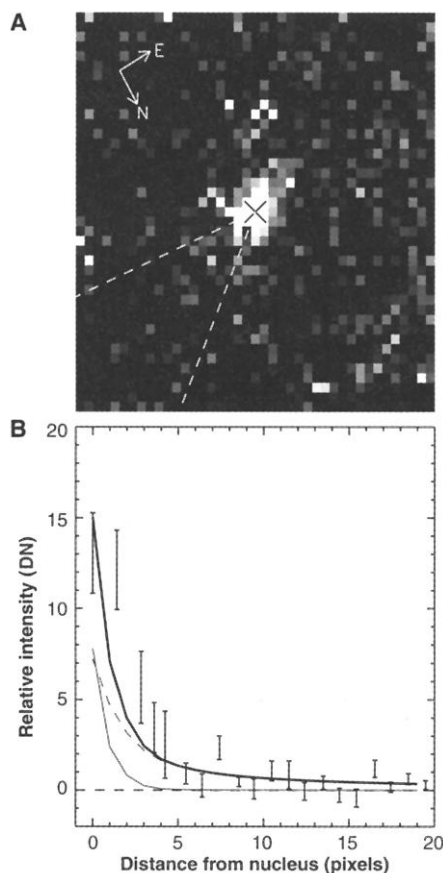


Fig. 4. Individual fragment and its spatial brightness profile. (A) The HST PC image of fragment K, with the estimated position of the nucleus marked (cross near center of image). (B) The spatial brightness profile for the region between the dashed lines in (A) (30° acute angle). This region is centered on the sunward direction and was selected to avoid tailward moving debris. The compass shows the directions of celestial north and east, and the width of the entire image is 1.87 arc sec. The data and their error bars (1σ) are plotted along with our best fit model (22) for the nucleus contribution (thin solid curve), the coma contribution (dashed curve), and the sum of the two (thick solid curve). The nucleus contributes about half of the observed signal in the peak pixel, and its corresponding R-band magnitude is ~ 26 . DN, data numbers.

Thus, we must look to other physical mechanisms, such as fast rotation (30) or collisions with asteroidal debris (31), possibly combined with increased activity associated with the comet's approach to perihelion, as possible triggers for the unraveling of C/LINEAR.

References and Notes

1. J. Chen, D. Jewitt, *Icarus* **108**, 265 (1994).
2. Z. Sekanina, in *Comets*, L. L. Wilkening, Ed. (Univ. of Arizona Press, Tucson, 1982), pp. 251–287.
3. ———, *Icarus* **58**, 81 (1984).
4. ———, *Astron. Astrophys.* **318**, L5 (1997).
5. M. Kidger et al., *IAU Circ.* **7467** (2000) (available at <http://cfa-www.harvard.edu/iauc/07400/07467.html>).
6. G. H. Stokes, J. B. Evans, H. E. M. Vigg, F. C. Shelly, E. C. Pearce, *Icarus* **148**, 21 (2000).
7. J. H. Oort, *Bull. Astron. Inst. Neth.* **11**, 91 (1950).
8. P. R. Weissman, in *Completing the Inventory of the Solar System*, T. W. Rettig, J. M. Hahn, Eds., vol. 107 of *ASP Conference Series* (Astronomical Society of the Pacific, San Francisco, 1996), pp. 265–288.
9. The STIS is used for spectroscopic and imaging observations spanning the wavelength range from ~110 to ~1100 nm. Our imaging observations of C/LINEAR were made using the STIS CCD with its F28X50LP filter, which passes light between ~550 and ~1100 nm. The CCD pixels are square and are 0.050 arc sec on a side, which projects to 29 km at a distance of 0.8 AU. Our spectroscopic observations of C/LINEAR employed the G140L, G230L, G230LB, and G430M gratings. Further information on STIS is available at www.stsci.edu/instruments/stis/.
10. The acceleration of an object from solar gravity, a_{solar} , is given by $a_{\text{solar}} = GM_{\odot}r_n^{-2} = 5.9 \times 10^{-3} r_n^{-2} \text{ m s}^{-2}$, where G is the gravitational constant, M_{\odot} is the mass of the Sun, and r_n is the object's heliocentric distance in AU.
11. The 2.2-m telescope located on the summit of Mauna Kea, on the island of Hawaii, is owned and operated by the University of Hawaii. We took images of C/LINEAR using the Tektronix 2048 by 2048 pixel CCD (Tek2K) (0.22 arc sec pixel⁻¹) with an R-band filter having a central wavelength of 646 nm and a bandpass of 125 nm.
12. M. L. Finson, R. F. Probstein, *Astrophys. J.* **154**, 353 (1968).
13. The acceleration of a spherical dust particle by solar radiation pressure, a_{rad} , is given by $a_{\text{rad}} = 0.75Q_{\text{pr}}F_{\odot}/c\rho r_p$, where s is the radius of the particle, Q_{pr} is the scattering efficiency factor averaged over the solar spectrum, F_{\odot} is the solar flux integrated over wavelength at a heliocentric distance of 1 AU, c is the speed of light in vacuum, ρ is the particle's density, and r_p is the particle's heliocentric distance. Combining this expression with our previously defined expression for the acceleration due to solar gravity (10), we derive that β is given by $\beta = a_{\text{rad}}/a_{\text{solar}} = 0.57Q_{\text{pr}}/s\rho$ (s is in micrometers, and ρ is in g cm⁻³). Q_{pr} varies with particle size and composition but is usually within a factor of 2 of unity for particles with radii larger than a few tenths of a micrometer.
14. N. Divine et al., *Space Sci. Rev.* **43**, 1 (1986).
15. J. T. T. Mäkinen, J.-L. Bertaux, M. R. Combi, E. Quémerais, *Science* **292**, 1326 (2001).
16. D. Bockelée-Morvan et al., *Science* **292**, 1339 (2001).
17. The density of a cometary nucleus has never been measured directly, and various indirect techniques generally only poorly constrain the value. Nevertheless, most cometary researchers adopt a value that is considerably smaller than 1 g cm⁻³ because of the obvious fragility of many cometary nuclei.
18. The WFPC2 consists of three wide-field (WF) mode CCDs and one PC CCD arranged in a mosaic. The plate scales are 0.0996 arc sec pixel⁻¹ for the WF CCDs and 0.0455 arc sec pixel⁻¹ for the PC CCD. For all of our C/LINEAR observations, we used the F675W filter, which has a mean wavelength of 668 nm, an effective width of 87 nm, and, among the WFPC2 filters, is the closest in transmission properties to the standard astronomical R band. The cometary emissions transmitted by the F675W filter are dominated by the scattering of sunlight by cometary dust, as there are no strong cometary gaseous emissions in the bandpass of the filter. The point spread function of the PC has a full width at half maximum of ~0.070 arc sec, which projects to 40 km at a geocentric distance of 0.8 AU. The resolution achieved during the C/LINEAR observations was similar, as HST was programmed to follow the track of the comet and did so with an accuracy of ~0.015 arc sec (root-mean-square error). Further information on the WFPC2 is available at www.stsci.edu/instruments/wfpc2/wfpc2_top.html.
19. The ephemeris for C/LINEAR became ambiguous after the late-July 2000 disruption event, as observers could no longer locate a strong brightness condensation to identify as the position of the comet's nucleus. Therefore, we used an orbit solution (JPL-87; this is equivalent to the orbital elements published by the International Astronomical Union [*IAU Minor Planets Circ.* 40988 (2000)]) that only included astrometric data through 22 July 2000, when a clear condensation was still visible, and targeted the predicted location of the nucleus as our highest priority. When astrometric data taken through 25 July 2000 are included in the orbit solution (JPL-95), the predicted position of the nucleus is ~20 arc sec east of the location predicted by the JPL-87 solution at the time of our August observations, as the astrometry became biased by the presence of the bright dust tail. Fragments breaking off from the nucleus will be accelerated in the antisolar direction (i.e., approximately due east) by jetting forces, and the most massive fragments are generally expected to be the westernmost ones.
20. The VLT is a facility that is owned and operated by the European Southern Observatory (ESO) and is located at the Paranal Observatory in Chile. For our observations of C/LINEAR, we used ANTU, one of four 8.2-m telescopes that will eventually be combined interferometrically, with the focal reducer/low dispersion spectrograph (FOR51). We used FOR51 in standard resolution imaging mode, which employs a CCD camera having 2048 by 2048 pixels and a plate scale of 0.2 arc sec pixel⁻¹, with the R_{best} filter, which has an effective wavelength of 657 nm, a width (full width at half maximum) of 150 nm, and is designed to mimic the transmission of the standard astronomical R band. The observations on 6 August were made under photometric conditions and an average seeing of ~0.6 arc sec. The seeing on 9 August was ~1.2 arc sec, and thin cirrus clouds and a bright Moon further degraded the observations. Processing of those data (21) showed three faint blobs at the expected position of the fragments, but no quantitative information could be obtained. The observational conditions on 14 August were comparable to the conditions on 6 August, yet processing of the images revealed only marginal evidence for a few fragments. Thus, by 14 August, the brightnesses of the fragments were at or below the VLT's sensitivity limit of $m_R \approx 27.5$, where m_R is the magnitude in the standard astronomical R band. Active tracking of the comet was employed for all of the VLT observations, and the estimated tracking error was ≤ 0.1 arc sec. Further information on FOR51 and the VLT is available at www.eso.org/instruments/fors1/.
21. The visibility of the fragments in the VLT images was substantially improved by subtracting a smoothed image from the original to remove the low-spatial-frequency (i.e., relatively smooth) component, a standard image-processing technique known as "unsharp masking." We also performed a wavelet analysis of the sharpened images to enhance the spatial frequency information associated with true unresolved astronomical sources while suppressing the pixel-to-pixel noise.
22. P. L. Lamy, I. Toth, H. A. Weaver, *Astron. Astrophys.* **337**, 945 (1998).
23. Z. Sekanina, *Earth Moon Planets* **77**, 147 (1999).
24. The WFPC2 CCD signal measured through the F675W filter and attributed to the nucleus was converted to an R magnitude in the Landolt-Kron-Cousins photometric system with $m_{\text{comet}} = -2.5 \log S + 22.07$, where m_{comet} is the R magnitude of the nucleus and S is the count rate of the nucleus (data number s⁻¹). Then the diameter of the nucleus, d_N (km), can be calculated with $d_N = [(2.99 \times 10^8) 10^{0.2(m_{\text{sun}} - m_{\text{comet}} + 5 \log r_A + 0.04\phi)}] / A_p^{0.5}$, where m_{sun} is the R magnitude of the Sun

(-27.10), A_p is the geometric albedo, and ϕ is the phase angle (Sun-comet-Earth angle).

25. A factor of 2 change in the phase law, which probably defines the extreme limits, produces a factor of ~2 change in the derived size. Although the albedo has not been measured for many cometary nuclei, all of the values lie within a factor of ~3 of 4% (32), the value determined for comet 1P/Halley (33). The size is inversely proportional to the square root of the albedo, so the uncertainty in albedo translates into a factor of ~1.7 uncertainty in the size. A potentially even larger source of systematic error is the difficulty in determining accurate magnitudes for such faint fragments embedded within dust comae. Certainly our size estimates for the fainter fragments listed in Table 2 are questionable, even though models using these magnitudes provide a better fit to the data than assuming that all of the observed flux is due to a dust coma. Finally, we note that an error of a factor of 2 in the sizes produces an error of a factor of 8 in the mass.
26. H. Weaver, *IAU Circ.* **7461** (2000) (available at <http://cfa-www.harvard.edu/iauc/07400/07461.html>).
27. We measured several emission bands of CO during observations between 5.78 and 5.94 July 2000 and used those data to derive a CO production rate of $\sim 5 \times 10^{26}$ molecules s⁻¹. We assumed that all CO was flowing outward from the nucleus with a speed of $0.8r_n^{0.5}$ km s⁻¹ and that the total CO lifetime was $1 \times 10^7 r_n^2$ s. The formal error in our CO production rate, including absolute calibration uncertainty, is ~20%, but various systematic effects (e.g., temporal variability, uncertainties in the outflow velocity and fluorescence efficiency factors, etc.) add a comparable amount of error. We measured several bands of OH during observations between 6.73 and 6.89 July 2000 and used those data to derive a water production rate of $\sim 1.2 \times 10^{29}$ molecules s⁻¹. We assumed that the H₂O outflow velocity was $0.8r_n^{0.5}$ km s⁻¹, that the total H₂O lifetime was $8.2 \times 10^4 r_n^2$ s, that 84% of the H₂O destruction produced OH, that the OH was ejected isotropically in the frame of the dissociating H₂O molecule with a velocity of 1.05 km s⁻¹, and that the OH lifetime was $1.6 \times 10^7 r_n^2$ s. As for CO, the formal error in our water production rate is ~20%, but systematic errors probably contribute a comparable amount. Because our CO observations were made during the course of a strong outburst in activity and the OH observations were made 1 day later during a period of declining activity, we regard our derived CO/H₂O abundance ratio as an upper limit. Mumma et al. (34) derived CO and H₂O production rates of $\sim (7 \pm 2) \times 10^{26}$ molecules s⁻¹ and $\sim (7.46 \pm 0.74) \times 10^{28}$ molecules s⁻¹, respectively, on 5.80 July 2000, on the basis of infrared observations (wavelength $\lambda \sim 4.67 \mu\text{m}$) of a single line in the CO (1,0) vibrational band and a single line in the H₂O $\nu_3 - \nu_2$ vibrational band.
28. W. Irvine, F. P. Schloerb, J. Crovisier, B. Fegley, M. J. Mumma, in *Protostars and Planets IV*, V. Mannings, A. P. Boss, S. S. Russell, Eds. (Univ. of Arizona Press, Tucson, 2000), pp. 1159–1200.
29. T. Yamamoto, in *Comets in the Post-Halley Era*, R. A. Newburn, M. Neugebauer, J. Rahe, Eds. (Kluwer, Dordrecht, Netherlands, 1991), pp. 361–376.
30. T. L. Farnham et al., *Science* **292**, 1348 (2001).
31. I. Toth, *Astron. Astrophys.* **368**, L25 (2001).
32. Y. R. Fernandez et al., in *Cometary Nuclei in Space and Time*, M. F. A'Hearn, Ed., (Astronomical Society of the Pacific, San Francisco, in press).
33. H. U. Keller, N. Thomas, *Adv. Space Res.* **19**, 187 (1997).
34. M. J. Mumma et al., *Science* **292**, 1334 (2001).
35. We thank the directors of the Space Telescope Science Institute (STScI) and the ESO/VLT for approving our programs for Director's Discretionary Time. We also express our sincere appreciation to the telescope operations teams of the HST and VLT for their excellent support of these target-of-opportunity observations in a timely manner. We thank P. Capak for making the University of Hawaii observations on 5 August 2000. Financial support for this work was provided by NASA through grant NAG5-4495 and through grants HST-GO-08276 and HST-GO-08876 from the STScI, which is operated by the Association of Universities for Research in Astronomy, under NASA contract NASS-26555.

26 December 2000; accepted 28 March 2001